

Modeling Solid Rocket Booster Exhaust Plumes in the Stratosphere with SURFACE CHEMKIN

1 September 1995

Prepared by

B. B. BRADY and L. R. MARTIN
Mechanics and Materials Technology Center
Technology Operations

Prepared for

SPACE AND MISSILE SYSTEMS CENTER
AIR FORCE MATERIEL COMMAND
2430 E. El Segundo Boulevard
Los Angeles Air Force Base, CA 90245

Engineering and Technology Group

19960920 026

APPROVED FOR PUBLIC RELEASE;
DISTRIBUTION UNLIMITED

DTIC QUALITY INSPECTED 3

This report was submitted by The Aerospace Corporation, El Segundo, CA 90245-4691, under Contract No. F04701-93-C-0094 with the Space and Missile Systems Center, Los Angeles Air Force Base, 2430 E. El Segundo Blvd., Los Angeles, CA 90245. It was reviewed and approved for The Aerospace Corporation by S. Feuerstein, Principal Director, Mechanics and Materials Technology Center. John Edwards was the project officer for the program.

This report has been reviewed by the Public Affairs Office (PAS) and is releasable to the National Technical Information Service (NTIS). At NTIS, it will be available to the general public, including foreign nationals.

This technical report has been reviewed and is approved for publication. Publication of this report does not constitute Air Force approval of the report's findings or conclusions. It is published only for the exchange and stimulation of ideas.



John Edwards
SMC/CEV

REPORT DOCUMENTATION PAGE

Form Approved
OMB No. 0704-0188

Public reporting burden for this collection of information is estimated to average 1 hour per response, including the time for reviewing instructions, searching existing data sources, gathering and maintaining the data needed, and completing and reviewing the collection of information. Send comments regarding this burden estimate or any other aspect of this collection of information, including suggestions for reducing this burden to Washington Headquarters Services, Directorate for Information Operations and Reports, 1215 Jefferson Davis Highway, Suite 1204, Arlington, VA 22202-4302, and to the Office of Management and Budget, Paperwork Reduction Project (0704-0188), Washington, DC 20503.

1. AGENCY USE ONLY (Leave blank)	2. REPORT DATE 1 Sept 1995	3. REPORT TYPE AND DATES COVERED
4. TITLE AND SUBTITLE Modeling Solid Rocket Booster Exhaust Plumes in the Stratosphere with SURFACE CHEMKIN		5. FUNDING NUMBERS F04701-93-C-0094
6. AUTHOR(S) B. B. Brady and L. R. Martin		
7. PERFORMING ORGANIZATION NAME(S) AND ADDRESS(ES) The Aerospace Corporation Technology Operations El Segundo, CA 90245-4691		8. PERFORMING ORGANIZATION REPORT NUMBER TR-95(5231)-9
9. SPONSORING/MONITORING AGENCY NAME(S) AND ADDRESS(ES) Space and Missile Systems Center Air Force Materiel Command 2430 E. El Segundo Boulevard Los Angeles Air Force Base, CA 90245		10. SPONSORING/MONITORING AGENCY REPORT NUMBER SMC-TR-96-19
11. SUPPLEMENTARY NOTES		
12a. DISTRIBUTION/AVAILABILITY STATEMENT Approved for public release; distribution unlimited		12b. DISTRIBUTION CODE
13. ABSTRACT (Maximum 200 words) The results of a detailed chemical model of the transient stratospheric chemistry following passage of a large solid rocket booster motor is described. The model is based on SURFACE CHEMKIN, which is a newly developed multiphase chemical kinetic model. The model incorporates 34 chemical species and over 100 gas phase, heterogeneous, and photochemical reactions. The results show that passage of a Titan IV-sized rocket should produce an ozone "hole" 10 km in diameter at 20 km altitude, and 28 km in diameter at 30 km altitude, lasting from a few hours to a day. The size and persistence of the hole are very sensitive to the rate of dissipation of the rocket plume, which is poorly understood at present.		
14. SUBJECT TERMS Stratospheric chemistry, ozone hole, Titan IV, rocket plume		15. NUMBER OF PAGES 29
		16. PRICE CODE
17. SECURITY CLASSIFICATION OF REPORT UNCLASSIFIED	18. SECURITY CLASSIFICATION OF THIS PAGE UNCLASSIFIED	19. SECURITY CLASSIFICATION OF ABSTRACT UNCLASSIFIED
20. LIMITATION OF ABSTRACT		

Contents

1. Introduction.....	1
2. Background.....	1
3. Comparison with Chlorofluorocarbons	3
4. Potential Heterogeneous Reactions	3
5. Model Description	4
6. Input Data for the Computations.....	6
7. Description of Results.....	6
8. Conclusions	8
9. Recommendations	9
References	28
Appendix A	A-1

Figures

1. Far-field Chemical Identity of Chlorine As a Function of Altitude	14
2. Starting Conditions—20 km	15
3. Starting Conditions—30 km	16
4. Ozone Depletion at 20 km, Full Reaction Mechanism.....	17
5. Ozone Depletion at 30 km, Full Reaction Mechanism.....	18
6. Ozone Depletion at 20 km, No Photolysis	19
7. Ozone Depletion at 20 km, Gas Phase Chlorine Reactions Only.....	20
8. Ozone Depletion at 20 km, NO, and Surface Only.....	21
9. Ozone Depletion at 20 km, Surface Reactions Only.....	22
10. Ozone Depletion at 20 km, All Chlorine as HCl, No NO _x	23
11. Ozone Depletion at 20 km at Three Sticking Coefficient Surface Reactions	24
12. Ozone Hole Persistence As a Function of HCl Dissipation Time	25
13. Ozone Hole Diameter As a Function of HCl Dissipation Time	26
14. Trimodal Size Distribution of Alumina Particles.....	27

Tables

Kinetic Data	10
--------------------	----

1. Introduction

In this paper, we model the time evolution of a point on the centerline of a dispersing plume from a solid fuel rocket booster (in particular, a Titan IV rocket) in the stratosphere. We will do this at two altitudes—20 km and 30 km—to look for the transient effect on the stratospheric ozone layer. At this writing, there are some other papers in the literature (Refs. 1, 2, 3, 4) modeling this phenomenon, but the earlier papers do not include the effects of chlorine oxide dimer reactions on the ozone, and the Denison, et al., paper is for a much smaller rocket and uses a smaller set of chemical reactions. Our reaction set is based on a survey of several literature models of stratospheric chemistry, and we believe that the gas phase reaction set is complete to the extent of present knowledge. Our starting point will be the conditions predicted by the JANAF plume code at 2 seconds after passage of the rocket (see Zittel, Ref. 5). At this time, there will be a considerable amount of free Cl and Cl₂ from afterburning of the plume in the atmosphere. Figure 1, quoted from Zittel, shows the fraction of HC1 converted to active form as a function of altitude. This figure is based on the chemistry taking place 0–2 seconds after passage of the exit plane. The plume temperatures covered by the Zittel model range from about 2,000 K down to 400 K. We will compute the subsequent (2 seconds to 10 days) (400 K to ambient temperature) altitude dependent reactions of chlorine, nitrogen, and hydrogen oxides that occur in the reactively mixing plume. We will then discuss the implications of the model results and give some conclusions and recommendations for increasing our understanding of this transient phenomenon.

2. Background

Hydrogen chloride (HC1) is a major combustion product of solid rocket boosters that use ammonium perchlorate oxidizer. As this gas leaves the motor, plume models run at Aerospace and elsewhere (Refs. 1, 5) indicate that afterburning takes place, converting a substantial amount of the HC1 to Cl and Cl₂ (21–5%, depending on altitude). This occurs through reactions such as:



The chlorine so released will immediately react with ozone to begin a catalytic destruction cycle. At high altitudes (30 km, for example), the sequence will be:



At low altitudes (e.g., 20 km), a more complex ozone destruction cycle may take place involving the chlorine oxide dimer $(ClO)_2$ (Ref. 6):



This cycle is similar to that which causes the Antarctic ozone hole, except that the chlorine oxide dimer forms because of the high concentrations of chlorine in the rocket plume, and not because of low temperatures. Also, as we discovered in running this model, the principal route for generation of atomic chlorine from the dimer is not photolysis of the dimer (which is the route in the Antarctic) but the branched chain reaction of the dimer with atomic chlorine as shown above. Since the two reaction cycles shown above regenerate atomic chlorine, these cycles will continue to destroy ozone until the Cl and ClO return to HC1 by reactions with hydrogen-containing molecules such as methane or hydrogen:

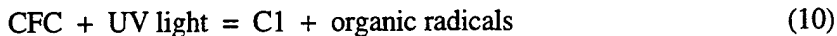


In the normal stratosphere, the Cl and ClO are typically converted to HC1 by this process in a few days, with the HC1 returning only very slowly to active form. In a rocket plume, however, there is sufficient Cl and ClO so that substantial local depletion of ozone may take place on shorter time scales. There is some early observational evidence that a local ozone hole may be created (Ref. 7).

There is a very slow mixing of the stratosphere with the troposphere, so that over a period of several years, HC1 released into the stratosphere will eventually return to the troposphere and rain out, with an average characteristic time of a few years.

3. Comparison with Chlorofluorocarbons

During the time it takes for HC1 to diffuse back to the troposphere, it will spread over the globe, and one must consider how HC1 from rockets will compare with HC1 from chlorofluorocarbons (CFCs). A typical CFC has a very long lifetime in the troposphere, and since the troposphere contains about 95% of the mass of the atmosphere, 95% of a typical CFC resides passively in the troposphere. At any given time, the 5% present in the stratosphere is slowly photolyzing into atomic chlorine:



The chlorine atoms produced by photolysis will enter ozone destruction cycles as described above. Because CFCs have been produced for many years, the total amount in the atmosphere is on the order of 25 million tons, and about 300,000 tons of atomic chlorine are produced each year from photolysis. Because of the long lifetime of CFCs, this production of atomic chlorine is expected to continue with a characteristic lifetime of about 60 years even in the absence of further manufacture and release of these molecules. In comparing stratospheric chlorine release from rockets with that from CFCs, the global effect is thus similar to a hypothetical CFC with a lifetime of a few years (Ref. 19).

4. Potential Heterogeneous Reactions

Neither the global nor local effects described above consider the potential additional effects of the particulate exhaust of the solid rocket boosters. At this time, any heterogeneous chemistry that takes place on the particles (mostly alumina and aluminum oxychloride) is poorly understood. Some reactions that have been proposed are:

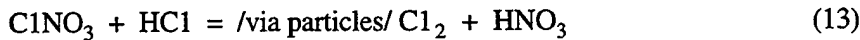
1. the direct destruction of ozone by surface catalysis:



2. catalysis of the photolysis of CFCs:



3. catalysis of reactions of "reservoir" species to put chlorine back into more reactive form, e.g.:



Reactions such as this are analogous to the reactions that take place on polar stratospheric clouds to produce the Antarctic ozone hole, but they are just beginning to be examined in the laboratory (see reference K at the end of the kinetics data table). The potential effect of such chemistry is one of the things we will examine.

5. Model Description

The computer model is based on the SURFACE CHEMKIN code developed by R. J. Kee of Sandia, Livermore (Refs. 8, 9, 10). This package contains subroutines for calculating thermodynamic properties, equilibrium constants, rates, and unit conversions, for parsing character data such as species and element names, and reaction mechanisms, and for solving the set of differential equations.

SURFACE CHEMKIN is a set of software tools and a subroutine library designed to help create a program to solve a specific chemical kinetics problem. The package is designed to solve a group of differential equations subject to a set of constraints; various properties of the system may be extracted along the way. One needs to write the program which describes the chemical system of interest, and calls the appropriate subroutines to do the calculations. Multiple surface and bulk phases can be included. Surface rates are scaled by the ratio of surface area to gas phase volume. The package is designed to model chemical vapor deposition. We wrote a driver program incorporating some changes in the calculation method, added some new subroutines, and modified some of the original routines. The resulting program is well adapted to atmospheric chemistry. Our alterations are described in more detail below.

The plume model is adiabatic. CHEMKIN calculates the enthalpy of each species in the model. As species are created or destroyed through reaction they add or subtract energy from the plume; mixing with the air also effects the energy balance. This net change in energy is divided by the heat capacity of the plume to obtain the temperature change for each integration step. This energy conservation equation is included as a governing equation, or constraint, for SURFACE CHEMKIN.

The governing equation for temperature, alluded to above, is based on conservation of energy, and is included here for reference.

$$\frac{\partial T}{\partial t} = \frac{\sum_{i=1}^N H_i^m m_i \left[\frac{\partial n_i^g}{\partial t} + \frac{\partial n_i^s}{\partial t} A_R + \frac{\partial n_i^\ell}{\partial t} V_R \right] + (T^{Air} - T) \frac{\partial \sigma_p}{\sigma_p \partial t} C_p^{Air}}{(C_p^g p + C_p^\ell m_\ell)}$$

The preceding equation describes the change in the plume temperature with time. The numerator in this equation is the total enthalpy change for the plume in time interval ∂t . The summation is over species i , where N is the total number of species considered; here N is 25. H_i^m is the enthalpy in mass units, m_i is the molecular weight of species i , and n_i^{phase} is the number of moles produced by gas, g , surface, s , or liquid phase, ℓ , reactions per unit volume (area for phase = s); the product $H_i^m m_i \frac{\partial n_i^g}{\partial t}$ represents

the heat gained or lost to the plume due to the production (or consumption) of a particular chemical species in gas phase reactions in the time interval ∂t . The rate of species production from surface reactions, $\frac{\partial n_i^s}{\partial t}$ is normalized by A_R , the ratio of surface area to gas phase volume. V_R is the ratio of liquid phase volume to gas phase volume, which normalizes the rate of species production from bulk phase reactions, $3 \frac{\partial n_i^\ell}{\partial t}$. T is the temperature, σ_p is the cross-sectional area of the plume, and C_p is heat capacity. The term $(T^{Air} - T) \frac{\partial \sigma_p}{\sigma_p \partial t} C_p^{Air}$ represents the heat required to bring ambient air, which is mixing into the plume, to the same temperature as the plume gases. The superscript *Air* refers to quantities in the undisturbed air outside the plume. The denominator in the above equation represents the specific heat of the plume and is made up of the specific heat of the gas phase, $C_p^g \rho$, and condensed phase, $C_p^\ell m_\ell$, portions, where ρ is the gas phase density, and the total mass in the liquid phase per unit volume of gas is m_ℓ . The heat capacity of the surface phase is negligible and is ignored.

The remaining constraints are based on conservation of mass and are broken down into separate equations for each species in each phase. The governing equation for gas phase species is:

$$\frac{\partial Y_i}{\partial t} = \frac{m_i}{\rho} \left[\frac{\partial n_i^g}{\partial t} + \frac{\partial n_i^s}{\partial t} A_R + \frac{\partial n_i^\ell}{\partial t} V_R \right] + \left(Y_i^{Air} - Y_i^g \right) \frac{\partial \sigma_p}{\sigma_p \partial t}$$

The symbol Y is used for the gas phase mass fraction. The first term in this equation is the molar changes due to reaction converted to a mass fraction, and the second term is the effect of dilution on plume species. This equation has a similar structure to the numerator of the first governing equation.

The equation for surface species in terms of site fraction, X_i , is similar. There is also a correction for coverage, where the density of surface sites in a given surface phase j is given by Γ_j and the number of sites occupied by a given species is σ_i . Large molecules could occupy several sites, but all the species in this model are small molecules with $\sigma_i = 1$. Only one surface phase (alumina/gas) is used in our model. There is an equation like the following one for each surface species.

$$\frac{\partial X_i}{\partial t} = \left(\frac{\partial n_i^s}{\partial t} + \frac{\partial n_i^\ell}{\partial t} V_R \right) \frac{\sigma_i}{\Gamma_j}$$

This complete set of constraints is used in solving the differential equations from the kinetics for each time step in the simulation.

To model the alumina particles we use a fixed condensed phase volume and surface area.

6. Input Data for the Computations

The model is formulated as a two bin system, consisting of a plume bin that slowly mixes with the surrounding stratosphere, and a stratosphere bin that is assumed to be infinite, i.e., concentrations of species in the overall stratosphere are assumed not to be perturbed by the plume. Interbin transport is described by a simple dilution function which gives the centerline concentration as a polynomial function of time. The dispersion (dilution) of the plume appears to be the most poorly understood part of this phenomenon at this time. We studied several different rates of dispersion to get an idea of the coupling between the chemistry and the dispersion, but most of the data presented is based on a dispersion model published by JPL (Ref. 11). This dispersion model was fit to a concentration that was a polynomial function of time. In all the runs, we include 0.01% helium in the initial plume as a "tracer" to show the rate of dilution. (The natural abundance of helium is omitted from the stratospheric bin for simplicity.)

The model includes 34 chemical species and some 100 gas phase chemical and photochemical reactions, and two heterogeneous reactions shown in Table 1 (see page 11). All the important stratospheric reactions of nitrogen, hydrogen, oxygen, and chlorine containing molecules are included. Heterogeneous reactions, including direct loss of ozone on alumina, and catalysis of the reaction of chlorine nitrate with HC1, are included as described in the results. Details of the parameters for this are given in Appendix A. The starting conditions at 20 km and 30 km are given in Figures 2 and 3, respectively. At 20 km altitude, the initial plume temperature is 400 K and the surrounding stratosphere is 217 K. At 30 km altitude, the initial plume temperature is 438 K and the surrounding stratosphere is 227 K. The starting conditions are based on a JANAF plume model (Ref. 5) for a Titan IV sized launch vehicle (Ref. 12). The hole sizes are based on the hydrogen chloride release rate of 2.0 tons per kilometer at 20 km altitude and 1.8 tons per kilometer at 30 km altitude (Ref. 6).

7. Description of Results

The model results are shown as log of the species concentrations *versus* log of the time, and temperature *versus* log of the time. Figure 4 shows the results at 20 km and Figure 5 the results at 30 km. These two figures are for the complete model, including heterogeneous chemistry, photochemistry, and chlorine and nitrogen oxide chemistry. It can be seen that the concentration of ozone is reduced by about a factor of 100 for about 10^4 seconds at 30 km altitude, and for about 2×10^4 seconds at 20 km. In each figure, the final ozone concentration is the ambient concentration and the final temperature is the ambient temperature.

Several features common to both curves deserve comment. First, for the initial hundred seconds less than 1% of the ozone remains. There is a partial resurgence of the ozone between 100 and 1,000 seconds. This appears to be related to the fall in temperature at this time as the cooling effect of stratospheric mixing is felt. There is also a pronounced peak in the OC1O and in the chlorine oxide dimer concentration after 10^4 seconds at both altitudes. This is due to the recovery in the ozone concentration, which rapidly reacts with any remaining C1. The disappearance of the C1 removes a

major sink for the dimer and so there is a resurgence in the concentration of the dimer between 10^4 and 10^5 seconds before final dispersal in the stratosphere.

Figure 6 shows the results at 20 km altitude with the photolysis reactions “turned off.” The primary effect here is that there are a few C1 atoms from the afterburning (see Figure 1), but no new formation of C1 atom; thus C1₂ accumulates. There is no catalytic cycle here; each C1 atom can destroy one ozone molecule at most before being ultimately tied up as (C1O)₂ or as C1₂. This stops the ozone destruction chemistry after 100 seconds, and the ozone recovers due to mixing with the ambient stratosphere beyond this time.

Figure 7 shows the results at 20 km altitude with heterogeneous chemistry and NO_x chemistry eliminated. The overall results are similar to the full reaction mechanism, as shown in Figure 4, indicating the dominance of gas phase chlorine chemistry in the plume. This is not surprising given that there is 10^7 times as much chlorine in the plume as in the ambient stratosphere, whereas there is only 10^4 times as much NO_x. The surface reactions require either ozone, which is already depressed by the gas phase reactions, or C1ONO₂, which is present at low concentrations in the ambient stratosphere and mixes slowly into the plume. Surface reactions may be important at longer times or at the plume edges where gas phase chlorine concentrations are smaller.

Figure 8 shows the results at 20 km altitude with no initial chlorine in the plume. The only chlorine species appearing in the calculations come from the ambient stratosphere. There is only slight ozone depletion due to NO_x chemistry, heterogeneous chemistry, and thermal decomposition. A comparison with Figure 7 confirms that gas phase chlorine chemistry dominates ozone loss in the plume. Interestingly, a comparison with Figure 6 shows the tremendous damage done by the chlorine atoms initially present in the plume during the first 100 seconds.

Figure 9 shows the results at 20 km altitude with no initial NO_x or chlorine in the plume. This is very similar to Figure 8, and shows that the small amount of ozone depletion seen is due to heterogeneous chemistry and thermal decomposition; NO_x does not contribute significantly to ozone depletion in the plume.

Figure 10 shows the results at 20 km altitude with all of the C1 initially in the form of HC1, i.e., with no “afterburning” of HC1. Interestingly, there is still some ozone depletion, although not nearly as much as in the afterburning case. Even beyond the afterburning region the OH in the plume is still much higher than in the ambient stratosphere. We attribute the ozone loss in this region to “cold” afterburning (i.e., below 400 K). (Note that there is still some atomic chlorine seen in this figure due to reaction of the HC1 with OH in the plume.)

Figure 11 shows double curves with, and without, heterogeneous chemistry, and with “enhanced” heterogeneous chemistry (see Table 1). It can be seen that including the heterogeneous chemistry can widen and deepen the ozone hole somewhat, but this requires a heterogeneous reactivity about 100 times higher than that seen in our laboratory experiments.

Figure 12 shows the effect of plume dispersion rate on the persistence of the “hole.” For these runs, a simple Gaussian dispersion in which the cross-sectional area of the plume increases as the square of time is used. Thus, the concentration of helium decreases with the square of time multiplied by a parameter. For our main runs, a polynomial in time was used (see above). It appears that the slower the dispersal, the longer the hole persists. There is very little experimental data on plume dispersion rates.

Figure 13 shows the approximate peak hole size as a function of dispersion rate, as described for Fig. 12. The hole size in this case is based on the total chlorine concentration at the time the ozone recovers, using the HC1 loadings from a Titan IV rocket (Ref. 12). The size of the hole depends to some degree on what is meant by ozone recovery; in this analysis, ozone is considered to recover when it reaches 30% of the ambient concentration.

8. Conclusions

The results of the detailed model calculations generally support our initial back-of-the-envelope calculations on the size of transient ozone holes created by passage of a solid rocket booster engine (Ref. 6). Since the plume dissipation rate is the most poorly understood part of this phenomenon, we treated this rate as a parameter to be varied over a wide range of values. The model has given the following information to date: 1) The peak hole size increases if the plume dissipates more slowly. The slowest rates of dissipation, which appear to be favored by the JPL model (Ref. 11), give a hole roughly 10 km in diameter at 20 km altitude, and 28 km in diameter at 30 km altitude. This result is somewhat counter-intuitive, and appears to be due to the second order nature of the chemistry involved. Since the formation of chlorine oxide dimer will depend on the square of the active chlorine concentration, the chain length for ozone destruction apparently also depends on the square of the concentration. Thus, a rapid dissipation of the plume will result in shorter chain lengths, and less overall ozone destruction. 2) Similarly, the slower the plume dissipates, the longer the hole persists, lasting from a few hours to a day. These model results suggest that dilution is the primary factor determining the effect of chlorine on ozone depletion. 3) Another interesting result is the importance of including chlorine oxide dimer, Cl_2O_2 , in the reaction scheme at lower altitudes such as 20 km. This species, which is of key importance in the formation of the Antarctic ozone hole, was omitted from most previous models of rocket plume chemistry. Inclusion of this species makes a significant difference in the hole size at 20 km altitude. 4) In addition, the model shows that photolysis of this species—neither the cross section nor the products are well established experimentally—(Refs. 20, 21, 22, 23) is *not* critical for ozone destruction in the first few hours (it may be important at later times or near the edges of the plume). In the special situation found in the plume center, it is reaction of the dimer with atomic chlorine that sustains the ozone destruction cycle.

9. Recommendations

The transient perturbation of the stratosphere by a passing rocket provides a unique opportunity to better our understanding of stratospheric chemistry, and to test our knowledge and theories. This preliminary work suggests that an observable local ozone depletion should take place, and studies of this phenomenon are important for understanding the environmental impact of launch vehicles and for basic knowledge of the atmosphere. We make the following recommendations for further work:

1. Sensitivity studies should be done to determine the gas phase rate coefficients most critical to determining the size and depth of the local ozone hole, and which need further laboratory study. These reactions may not be the same as those determining the steady state ozone concentration in the global stratosphere.
2. Similarly new heterogeneous reactions should be tested for importance in this phenomenon. Thus far only a handful of such processes have been considered.
3. New modeling studies of the potential global impact of rocket launches need to be done in view of our changing understanding of global ozone depletion. In particular, we refer to the newly discovered importance of heterogeneous reactions in the natural sulfate aerosol layer (the Junge layer), and the importance of redistribution of ozone depleted air from the Antarctic (Ref. 24). These effects account for a significant change in the predictions of current models, and may change the potential impact of rocket launches on the ozone layer as well.
4. Planning *in situ* and remote observations of this phenomenon must be done in concert with the predictions of a good model. Some spectroscopic studies by Beiting (Ref. 18) have already shown the importance of basing observational capabilities on realistic concentration predictions for the various species and their interferences. Further work is necessary for each new observational technique that is proposed.
5. The chemistry and photochemistry of chlorine oxide dimer, Cl_2O_2 , is of central importance to this phenomenon, as well as the Antarctic ozone hole. In our case, the photolysis is important at the edges of the hole, and at the time the hole begins to disappear. The chemical decomposition of the dimer is important at all times, and is not well documented.
6. The rate of mixing of the rocket plume with the surrounding atmosphere is poorly understood, yet the model calculations of ozone depletion are sensitive to this parameter. Measurements are needed to determine the rate of mixing and dissipation of the rocket plume.

We will be glad to collaborate with interested parties in developing work plans for pursuing each of these research topics.

Table 1. Kinetic Data

Elements

H O N Al C1 C He

Species

O2 N2 O O(1D) OH NO3 HO2 H2O2 C1 C1O CH3
 H2O NO NO2 O3 HC1 C1OO OC1O HOC1 C12 C12O2
 HNO3 N2O4 C1ONO2 H N N2O H2 HNO CO CO2
 HONO N2O5 CH4 He

Reactions

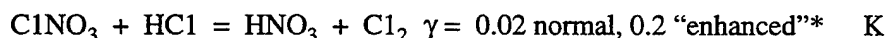
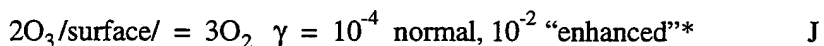
$k = AT^n e^{-Ea/RT}$ k units = $\text{cm}^3 \text{ molecule}^{-1} \text{ sec}^{-1}$, Ea in calories, for 3-body reactions, k in $\text{cm}^6 \text{ molecule}^{-2} \text{ sec}^{-1}$. Photochemical reactions are in sec^{-1} , at 20 km/30 km, as quoted in Reference B or calculated from the data therein. (Local noon, April 1, 40 N.) Photochemical reactions must be put into computer as irreversible, or the reverse reactions will be unrealistically speeded up by the thermodynamic program.

Reactants	Products	A	n	Ea(cal)	References
O3 + C1	= C1O + O2	2.9E-11	0	520	B
OH + C12	= HOC1 + C1	1.4E-12	0	1,790	B
O + HOC1	= OH + C1O	1.0E-11	0	4,370	B
C1 + O2 + M	=> C1OO + M	1.4E-29	-1.5	0	B
C1 + C1OO	= C12 + O2	2.3E-10	0	0	B
C1 + C1OO	= C1O + C1O	1.2E-11	0	0	B
C1 + HO2	= HC1 + O2	1.8E-11	0	-340	B
C1 + HO2	= OH + C1O	4.1E-11	0	890	B
C1O + HO2	= HOC1 + O2	4.8E-13	0	-1,390	B
C1O + O	= C1 + O2	3.0E-11	0	-140	B
O + C12	= C1O + C1	4.2E-12	0	2,720	G
C1 + H2O2	= HC1 + HO2	1.1E-11	0	1,950	A
O + C1OO	= C1O + O2	1.4E-10	0	0	H
OH + C1OO	= HOC1 + O2	1.4E-10	0	0	H
H + C1OO	= HC1 + O2	1.4E-10	0	0	H
O + O + M	= O2 + M	5.2e-35	0	-1,790	C
HO2 + NO	= NO2 + OH	3.7E-12	0	-477	A
O + NO2	= NO + O2	6.5E-12	0	-238	A
NO2 + H	= NO + OH	4.0E-10	0	675	B
NO + O	= N + O2	3.5E-15	1	38,747	D
O + N2	= NO + N	1.3E-10	0	75,506	E
N2O + M	= N2 + O + M	1.2E-6	-0.73	62,789	D
O + N2O	= N2 + O2	1.7E-10	0	28,017	D
N + NO2	= N2O + O	3E-12	0	0	B
N2O + H	= N2 + OH	1.6E-10	0	15,101	D
NO2 + H2	= HONO + H	3.98E-11	0	28,998	I
HNO + H	= H2 + NO	3E-11	0	994	D
HNO + OH	= H2O + NO	8E-11	0	994	D
NO + M	= N + O + M	2.4E-9	0	148,429	D

Reactants	Products	A	n	Ea(cal)	References
N2 + M	= N + N + M	3.82E5	-3.5	225,008	E
N + OH	= NO + H	3.8E-11	0	-169	A
C1O + NO	= NO2 + C1	6.4E-12	0	-576	B
HOC1 + OH	= H2O + C1O	3E-12	0	994	B
H2 + OH	= H2O + H	5.5E-12	0	3,974	B
OH + O	= H + O2	2.2E-11	0	-238	B
OH + H	= H2 + O	8.1E-21	2.8	3,875	C
OH + OH	= H2O + O	4.2E-12	0	477	B
OH + CO	= CO2 + H	1.5E-13	0	0	A
O3 + O	= O2 + O2	8E-12	0	4,093	B
O2 + hv	=> O + O	2.0E-13/3.0E-11	0	0	B
O + O2 + M	= O3 + M	3.0E-28	-2.3	0	B
O3 + hv	=> O + O2	6.0E-4/6.0E-4	0	0	B
O3 + hv	=> O(1D) + O2	3.0E-5/1.5E-4	0	0	B
O(1D) + H2O	= 2OH	2.2E-10	0	0	A
O(1D) + M	= O + M	2E-11	0	-213	A
O3 + HO2	= OH + O2 + O2	1.4E-14	0	994	B
OH + O3	= HO2 + O2	1.6E-12	0	1,867	B
OH + OH + M	= H2O2 + M	6.6E-29	-0.8	0	B
H + OH + M	= H2O + M	6.11E-26	-2.0	0	C
H + O2 + M	= HO2 + M	5.2E-28	-1.6	0	B
HO2 + OH	= H2O + O2	4.8E-11	0	-500	B
OH + H2O2	= H2O + HO2	2.9E-12	0	318	B
H + O3	= OH + O2	1.4E-10	0	954	B
H + HO2	= OH + OH	2.8E-10	0	874	C
H + HO2	= H2 + O2	1.1E-10	0	2,130	C
HO2 + HO2	= H2O2 + O2	2.2E-13	0	-1,190	A
O + HO2	= OH + O2	2.7E-11	0	-445	A
O + H2O2	= OH + HO2	1.4E-12	0	3,970	A
O3 + NO	= O2 + NO2	1.8E-12	0	2,720	A
NO3 + O	= NO2 + O2	1E-11	0	0	B
NO3 + NO	= NO2 + NO2	1.8E-11	0	-219	A
NO3 + OH	= NO2 + HO2	2.3E-11	0	0	A
NO3 + HO2	= NO2 + OH + O2	4.3E-12	0	0	A
OC1O + C1	= C1O + C1O	3.4E-11	0	-318	B
C12 + hv	=> C1 + C1	2.0E-3/2.0E-3	0	0	B
C1O + hv	=> C1 + O	1.0E-4/5.0E-4	0	0	B
C1OO + hv	=> C1O + O	.01/.01	0	0	B
OC1O + hv	=> C1O + O	.3/.3	0	0	B
HOC1 + hv	=> OH + C1	4E-4/5E-4	0	0	B
C1 + HOC1	= HC1 + C1O	3.0E-13	0	0	H
C1O + C1O + M	= C12O2 + M	8.7E-23	-3.9	0	B
C1O + O3	= C1OO + O2	1E-17	0	0	B
C1O + O3	= OC1O + O2	1E-12	0	7,948	B
OH + HC1	= H2O + C1	2.4E-12	0	656	A
OH + OC1O	= HOC1 + O2	4.5E-13	0	-1,590	A
OH + C1OO	= HO2 + C1O	1E-12	0	0	H

Reactants	Products	A	n	Ea(cal)	References
H ₂ O ₂ + C ₁ O	= HOC ₁ + HO ₂	1E-13	0	0	H
C ₁ 2O ₂ + C ₁	= C ₁₂ + C ₁ OO	1E-10	0	0	A
C ₁ 2O ₂ + hν	⇒ C ₁ 00 + C ₁	1.3E-3/1.7E-3	0	0	B
C ₁ O + NO ₂ + M	= C ₁ OMO ₂ + M	4.8E-23	-3.4	0	B
C ₁ ONO ₂ + C ₁	= C ₁₂ + NO ₃	6.8E-12	0	-318	A
C ₁ ONO ₂ + hν	⇒ C ₁ + NO ₃	6.0E-5/8.0E-5	0	0	B
C ₁ ONO ₂ + O	= C ₁ O + NO ₃	3.0E-12	0	1,589	A
C ₁ ONO ₂ + OH	= HOC ₁ + NO ₃	1.2E-12	0	655	A
C ₁ + CH ₄	= CH ₃ + HC ₁	9.6E-12	0	2,682.5	A
C ₁ + H ₂	= H + HC ₁	3.7E-11	0	4,570.1	A
O + OC ₁ O	= C ₁ O + O ₂	2.5E-12	0	1,888	A
OC ₁ O + NO	= NO ₂ + C ₁ O	2.5E-12	0	1,192	A
HC ₁ + O	= OH + C ₁	1.0E-11	0	6,636	A
H + C ₁ 2	= HC ₁ + C ₁	1.43E-10	0	1,172	G
2H + M	= H ₂ + M	1.5E-29	-1.3	0	C
2C ₁ + M	= C ₁₂ + M	6.14E-34	0	-1,800	G
H + O + M	= OH + M	1.3E-29	-1	0	C
CO + O + M	= CO ₂ + M	1.7E-33	0	3,000	C
NO + O + M	= NO ₂ + M	9.2E-28	-1.6	0	A
OH + NO ₂ + M	= HNO ₃ + M	2.6E-22	-3.2	0	B
H + NO + M	= HNO + M	2.47E-28	-1.3	735	D
OH + NO + M	= HONO + M	6.5E-25	-2.4	0	A
NO ₂ + O ₃	= NO ₃ + O ₂	1.2E-13	0	4,868	A
H ₂ O ₂ + hν	⇒ OH + OH	1.0E-5/1.5E-5	0	0	B
HO ₂ + hν	⇒ H + O ₂	1.0E-6/3.0E-6	0	0	B
NO ₂ + hν	⇒ NO + O	1.0E-2/1.0E-2	0	0	B
NO ₃ + hν	⇒ NO ₂ + O	0.3/0.3	0	0	B
NO ₃ + hν	⇒ NO + O ₂	0.03/0.03	0	0	A
HNO ₃ + hν	⇒ OH + NO ₂	1.0E-6/1.0E-5	0	0	B

Heterogeneous Reactions



* See description for Figure 11 in text.

References for Table 1 Kinetic Data

- A. R. Atkinson, D. L. Baulch, R. A. Cox, R. F. Hampson, Jr., J. A. Kerr, and J. Troe, "Evaluated Kinetic and Photochemical Data for Atmospheric Chemistry: Supplement IV," *Atmospheric Environment* **26A**, 1187–1230 (1992).
- B. W. B. DeMore, S. P. Sander, C. J. Howard, A. R. Ravishankara, D. M. Golden, C. E. Kolb, R. F. Hampson, M. J. Kurylo, and M. J. Molina, "Chemical Kinetics and Photochemical Data for Use in Stratospheric Modeling," Evaluation Number 10, JPL Publication, 92–20 (1992).
- C. W. Tsang and R. F. Hampson, "Chemical Kinetic Data Base for Combustion Chemistry. Part I. Methane and Related Compounds," *J. Phys. Chem. Ref. Data* **15**, No. 3, 1087–1280 (1986).
- D. W. Tsang and J. T. Herron, "Chemical Kinetic Data Base for Propellant Combustion. I. Reactions Involving NO, NO₂, HNO, HNO₂, HCN, and N₂O," *J. Phys. Chem. Ref. Data* **20**, No. 4, 609–663 (1991).
- E. D. J. Kewley and H. G. Hornung, "Free-Piston Shock-Tube Study of Nitrogen Dissociation," *Chem. Phys. Lett.*, **25**, 531 (1974).
- F. G. Brasseur and S. Solomon, *Aeronomy of the Middle Atmosphere*, Second Edition, D. Reidel Publishing Company, Holland (1986).
- G. D. L. Baulch, J. Duxbury, S. J. Grant, D. C. Montague, "Evaluated Kinetic Data for High Temperature Reactions. Volume 4. Homogeneous Gas Phase Reactions of Halogen- and Cyanide-Containing Species," *J. Phys. Chem. Ref. Data* **10**, Supplement No. 1, 721 pp. (1981).
- H. Estimate.
- I. M. W. Slack and A. R. Grillo, "Rate Coefficients for H₂ + NO₂ = HNO₂ + H Derived from Shock Tube Investigation of the H₂-O₂-NO₂ Ignition," *Combust. Flame* **31**, 275 (1978).
- J. A. O. Klimovski, A. V. Bavin, V. S. Tkalich, and A. A. Lisachenko, "Interaction of Ozone with γ -Al₂O₃ Surface," *React. Kinet. Catal. Lett.* **23**, 95–98 (1983). The value found in this paper is similar to that found in our preliminary laboratory experiments.
- K. R. Meads, D. D. Spencer, and M. J. Molina, "Stratospheric Chemistry of Aluminum Oxide Particles," Report to TRW Space and Technology Group (1994).

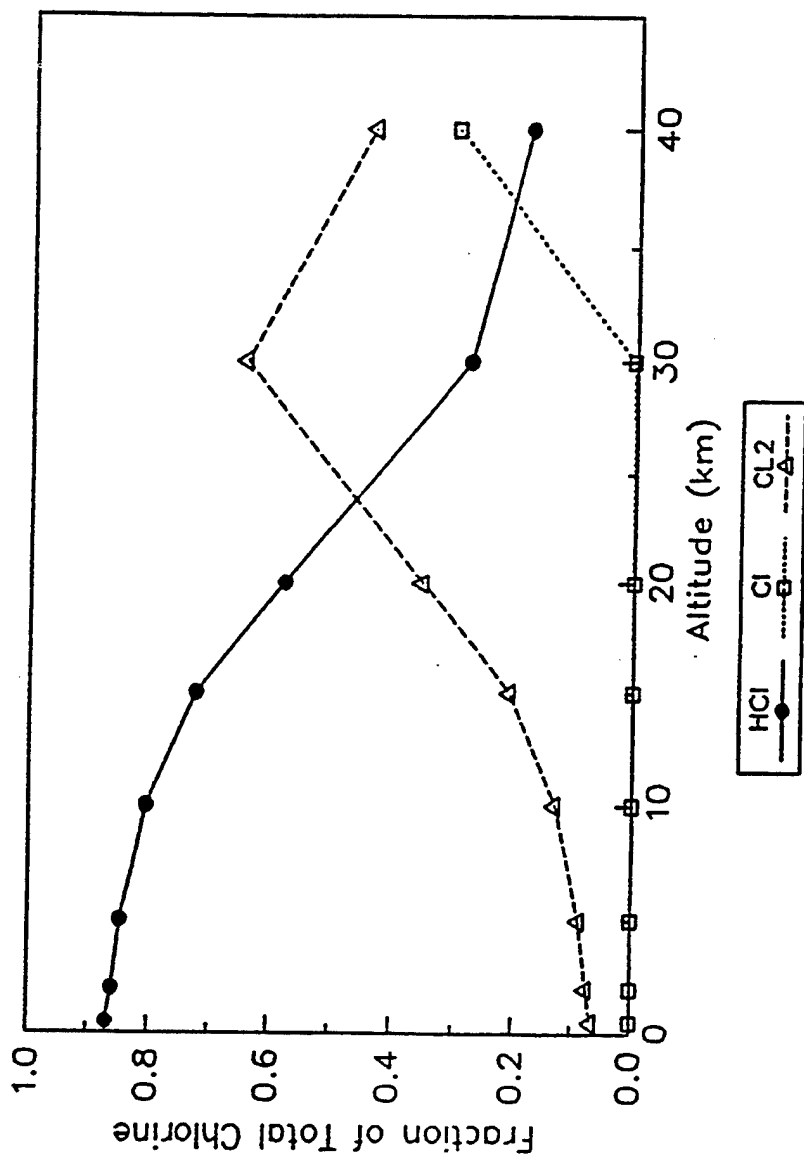


Figure 1. Far-field Chemical Identity of Chlorine as a Function of Altitude

- Plume
 - $P = 0.055$ atm, $T = 400.0$ K
 - Mole fractions: $N_2 = 0.78$, $O_2 = 0.18$, $H_2O = 0.022$, $CO_2 = 0.014$, $HCl = 4.1e-3$, $Cl_2 = 2.5e-3$, $OH = 5.4e-5$, $ClO = 2.8e-5$, $Cl = 7.2e-6$, $He = 1.0e-4$ (as a tracer).
- Stratosphere
 - $P = 0.055$ atm, $T = 217$ K
 - Mole fractions: $N_2 = 0.78$, $O_2 = 0.21$, $O_3 = 2.8e-6$, $CH_4 = 1.7e-6$, $H_2 = 1.1e-6$, $HCl = 6.1e-10$, $ClONO_2 = 2.0e-10$, $ClO = 1.5e-11$, $O = 8.3e-13$, $OH = 3.3e-13$, $Cl = 4.4e-16$.

Figure 2. Starting Conditions—20 km

- Plume
 - $P = 0.012 \text{ atm}$, $T = 438 \text{ K}$
 - Mole fractions: $N_2 = 0.78$, $O_2 = 0.20$, $H_2O = 0.012$, $CO_2 = 0.007$, $HCl = 1.1e-3$, $Cl_2 = 1.2e-3$, $OH = 2.2e-9$, $ClO = 3.1e-5$, $Cl = 1.5e-5$, $He = 1.0e-4$ (as a tracer).
- Stratosphere
 - $P = 0.012 \text{ atm}$, $T = 227 \text{ K}$
 - Mole fractions: $N_2 = 0.78$, $O_2 = 0.21$, $O_3 = 6.5e-6$, $CH_4 = 5.5e-7$, $H_2 = 4.7e-7$, $HCl = 1.3e-9$, $ClONO_2 = 1.3e-9$, $ClO = 3.9e-10$, $O = 1.6e-10$, $OH = 4.7e-12$, $Cl = 45.5e-14$.

Figure 3. Starting Conditions—30 km

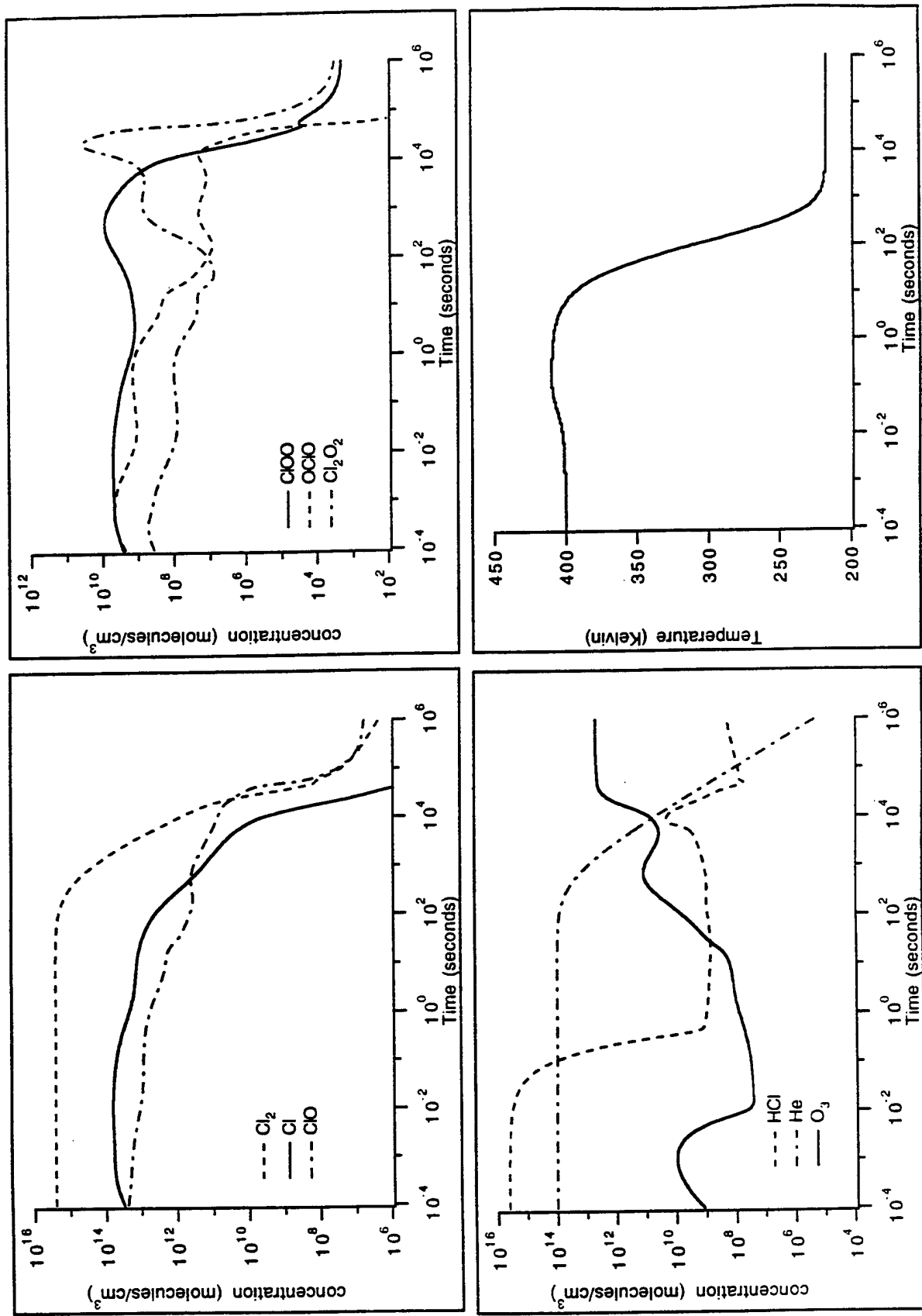


Figure 4. Ozone Depletion at 20 km, Full Reaction Mechanism

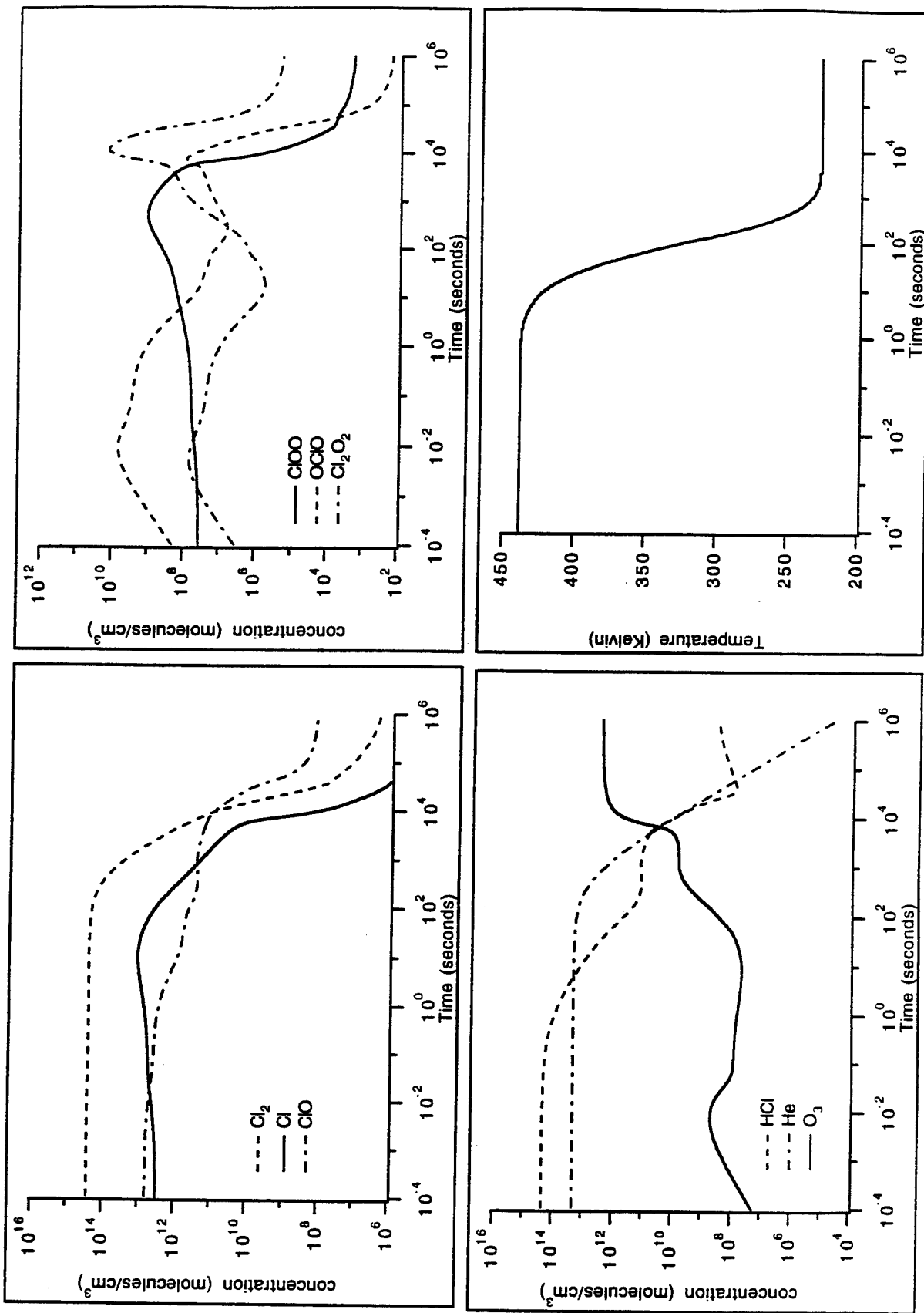


Figure 5. Ozone Depletion at 30 km, Full Reaction Mechanism

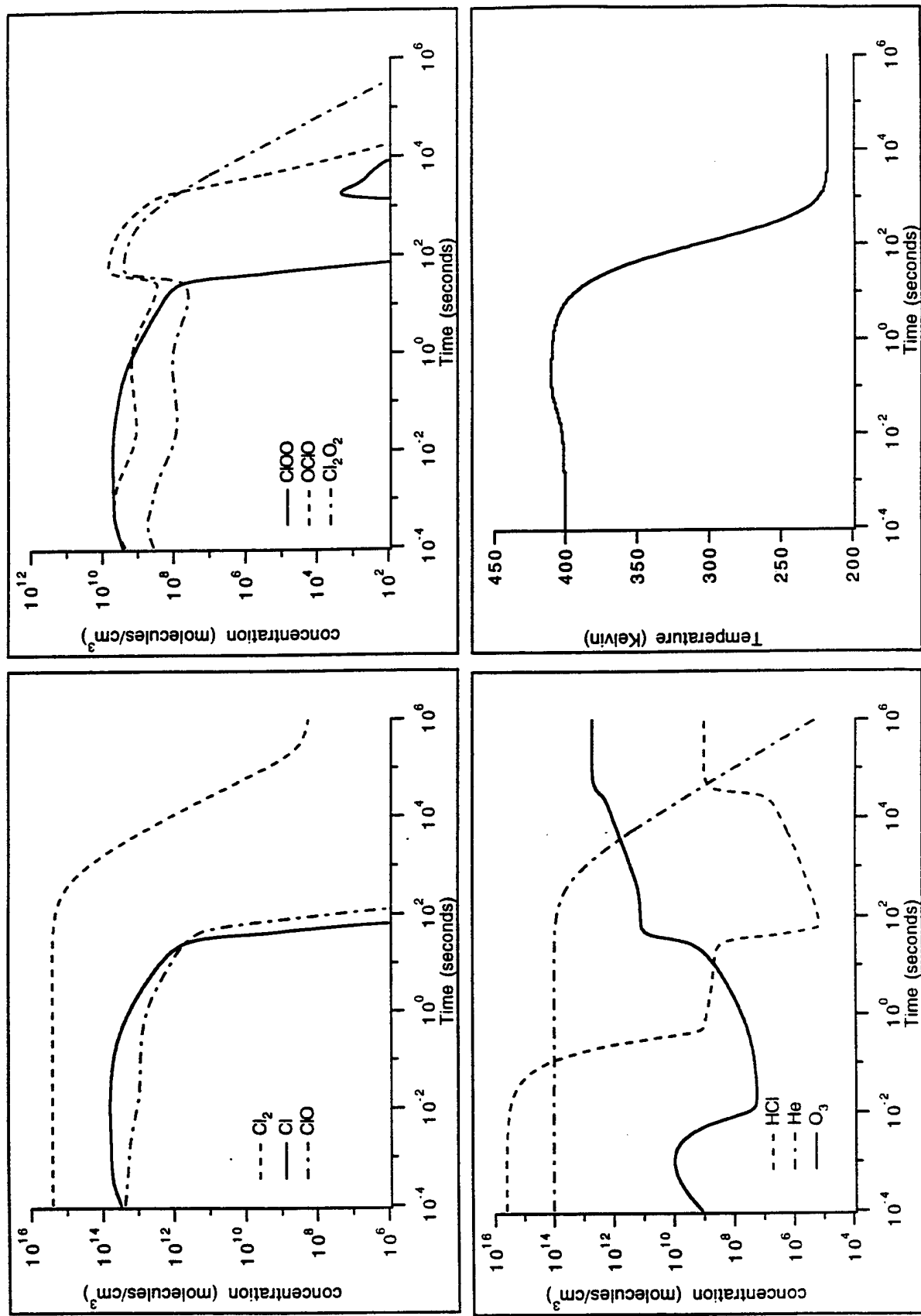


Figure 6. Ozone Depletion at 20 km, No Photolysis

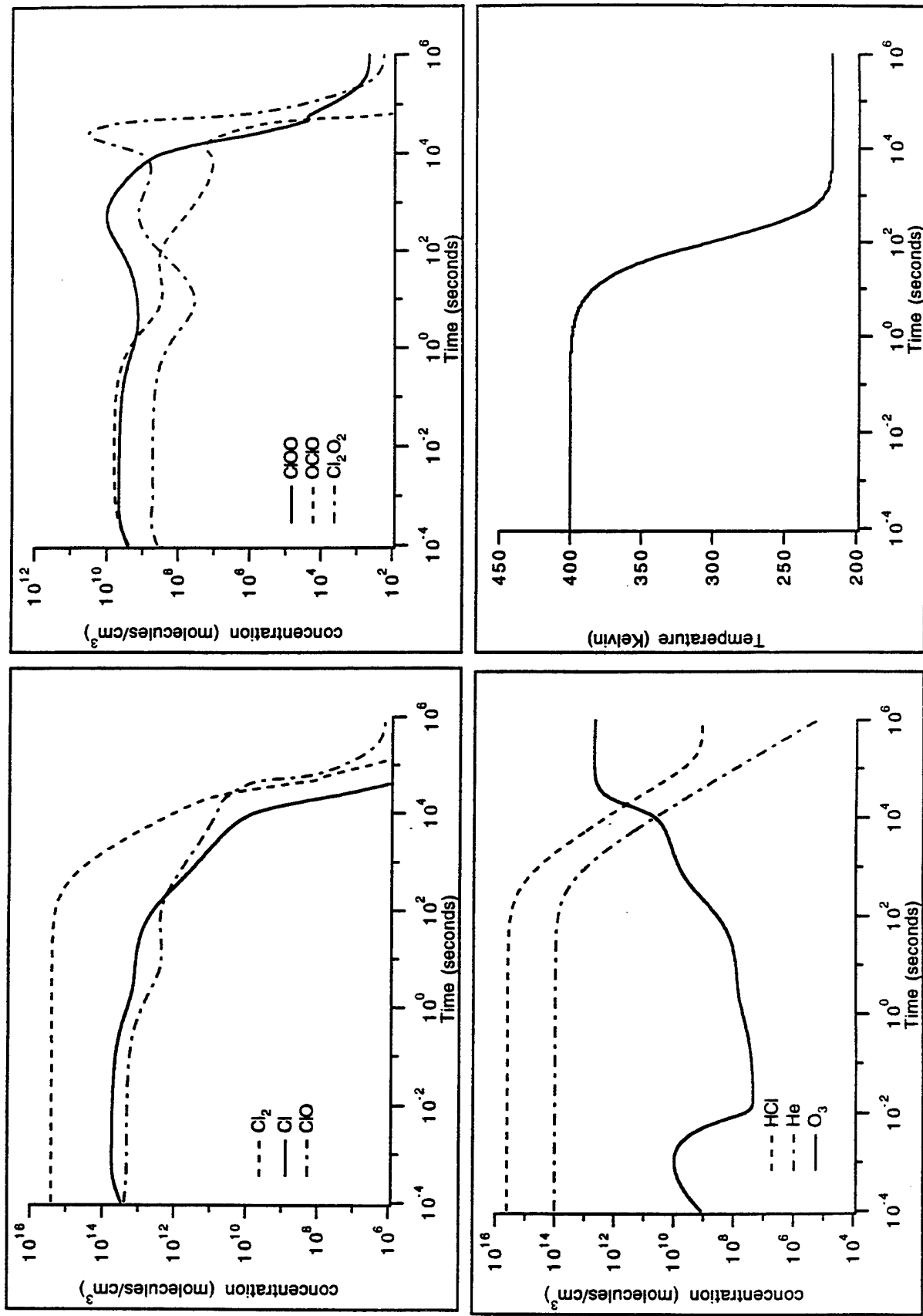


Figure 7. Ozone Depletion at 20 km, Gas Phase Chlorine Reactions Only

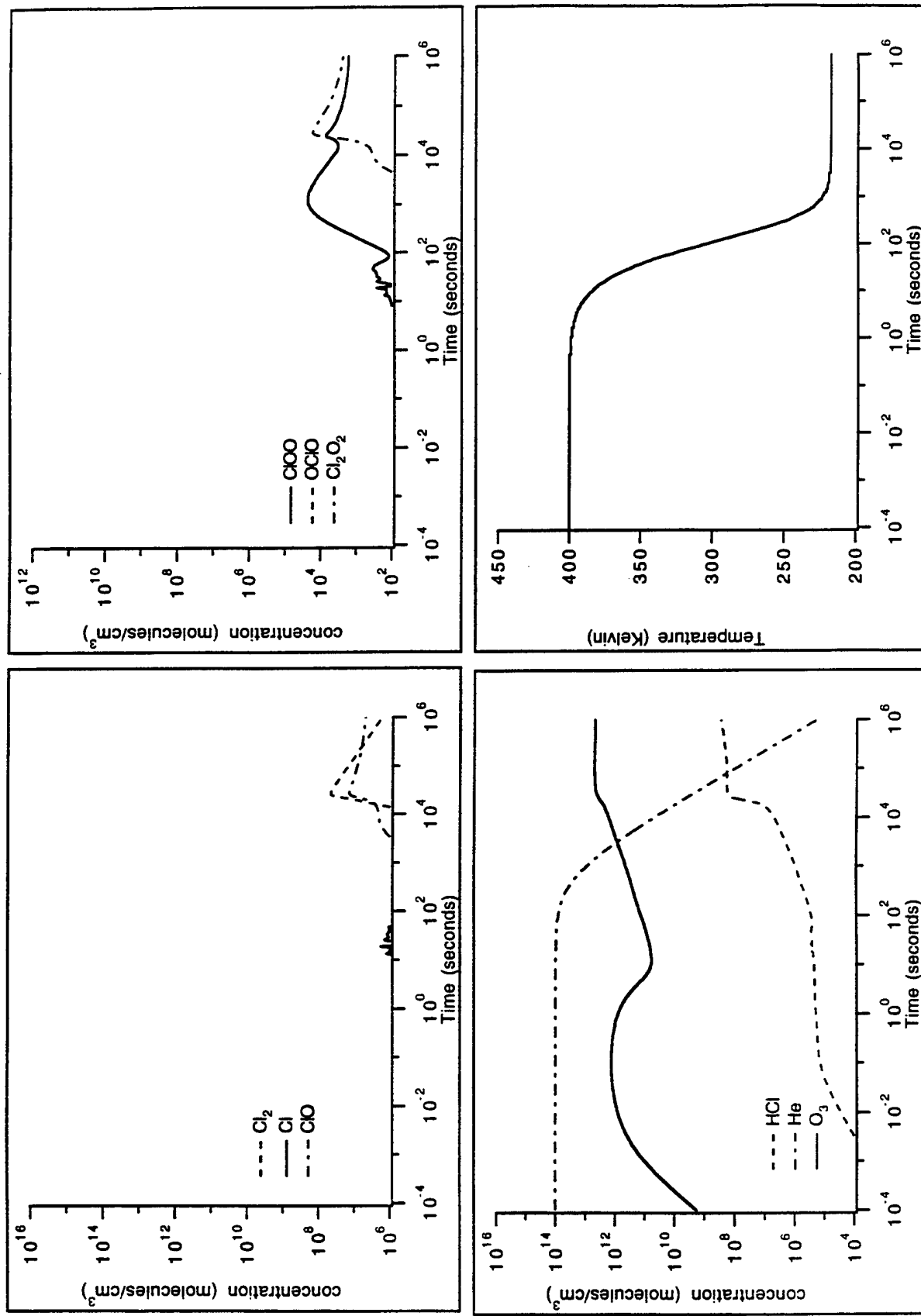


Figure 8. Ozone Depletion at 20 km, NO, and Surface Only

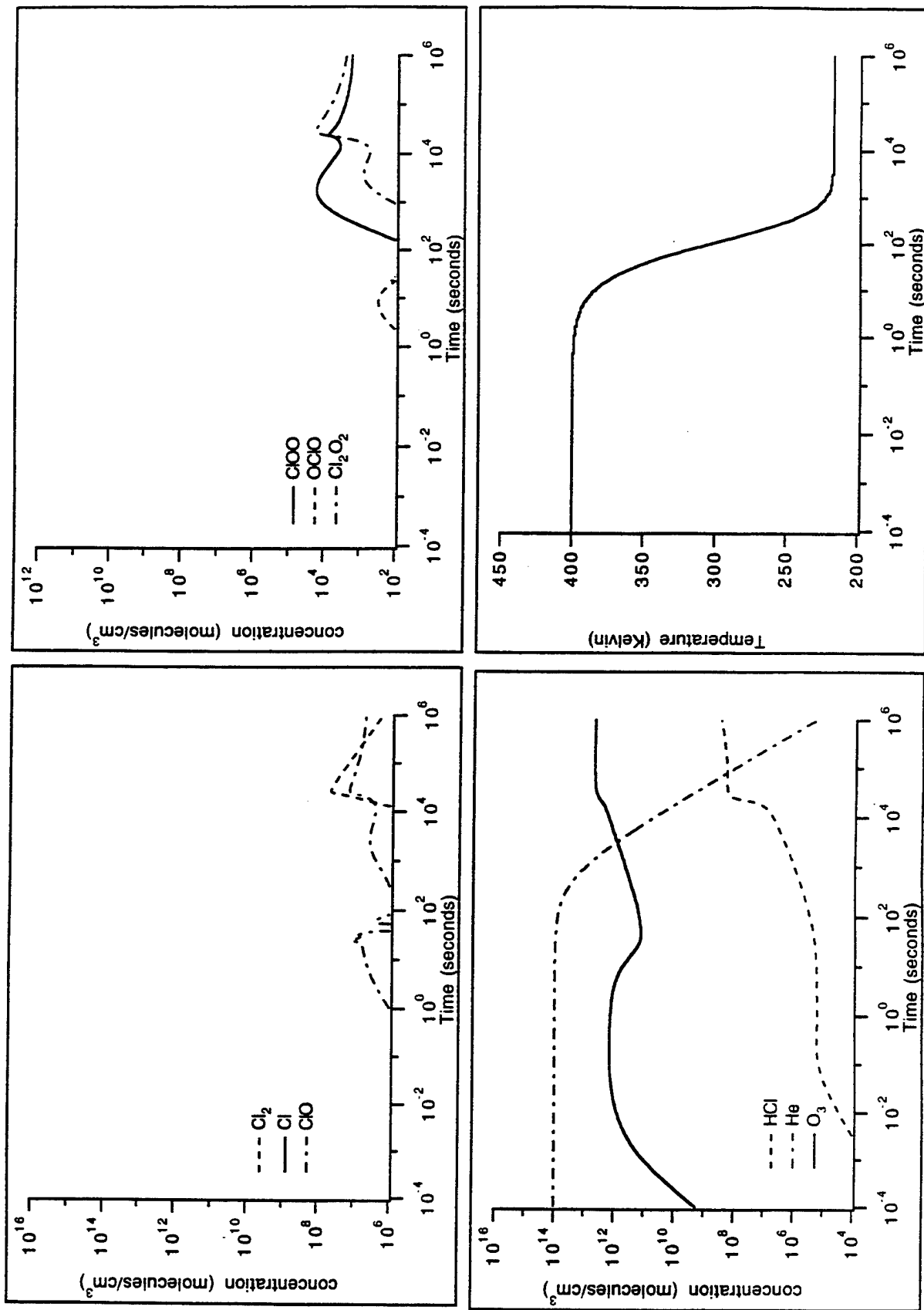


Figure 9. Ozone Depletion at 20 km, Surface Reactions Only

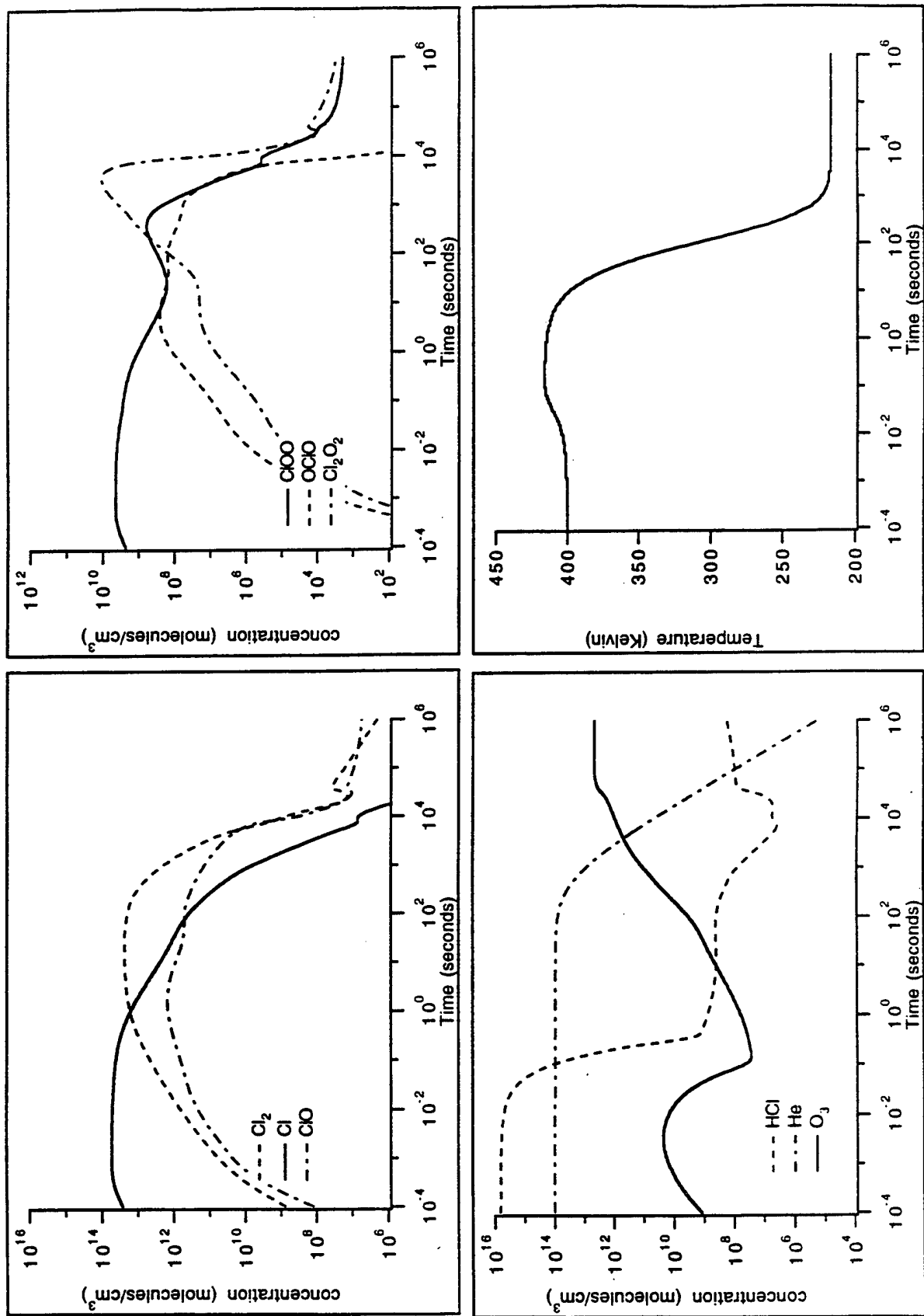


Figure 10. Ozone Depletion at 20 km, All Chlorine as HCl, No NO_x

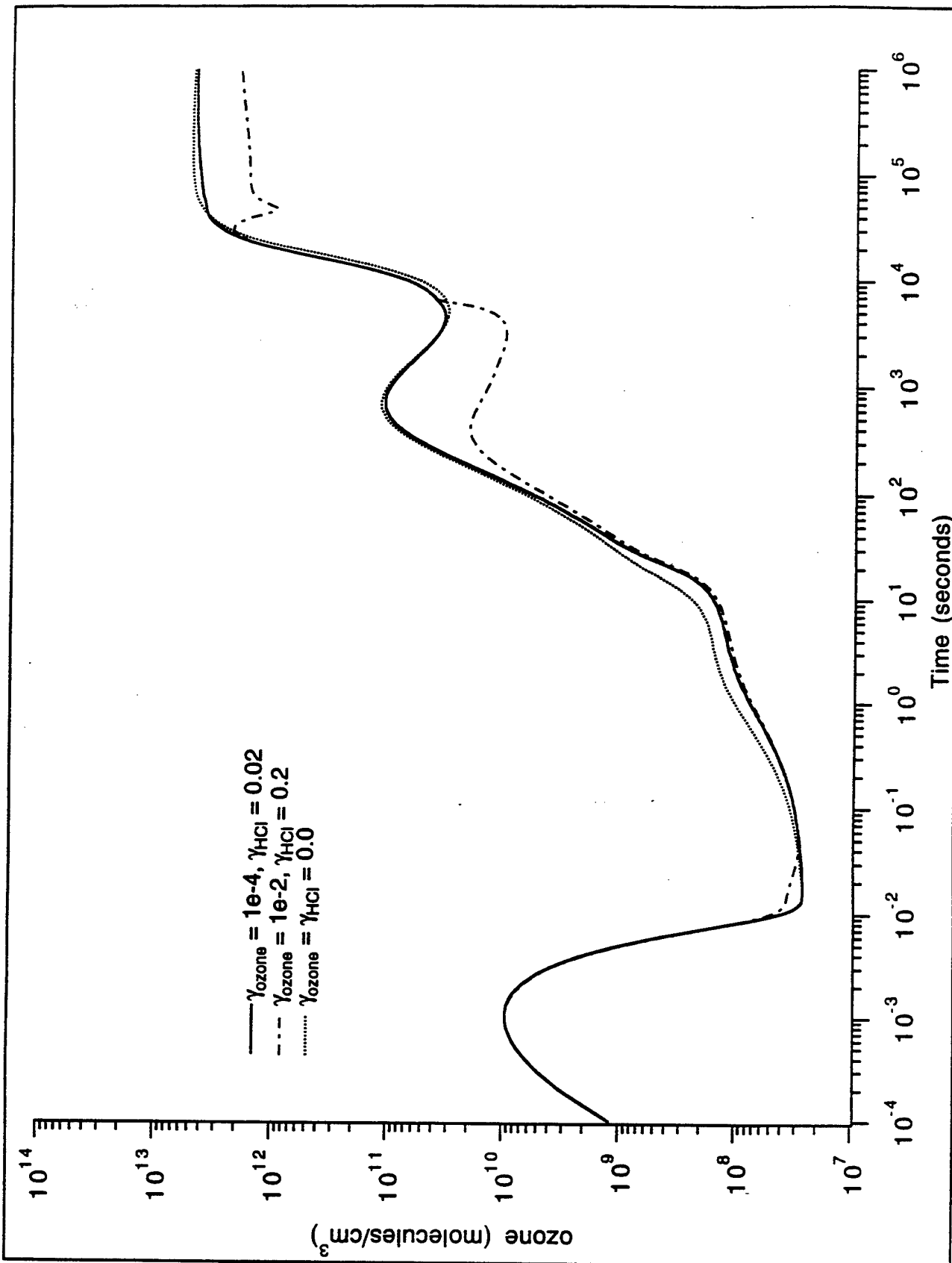


Figure 11. Ozone Depletion at 20 km at Three Sticking Coefficient for Surface Reactions

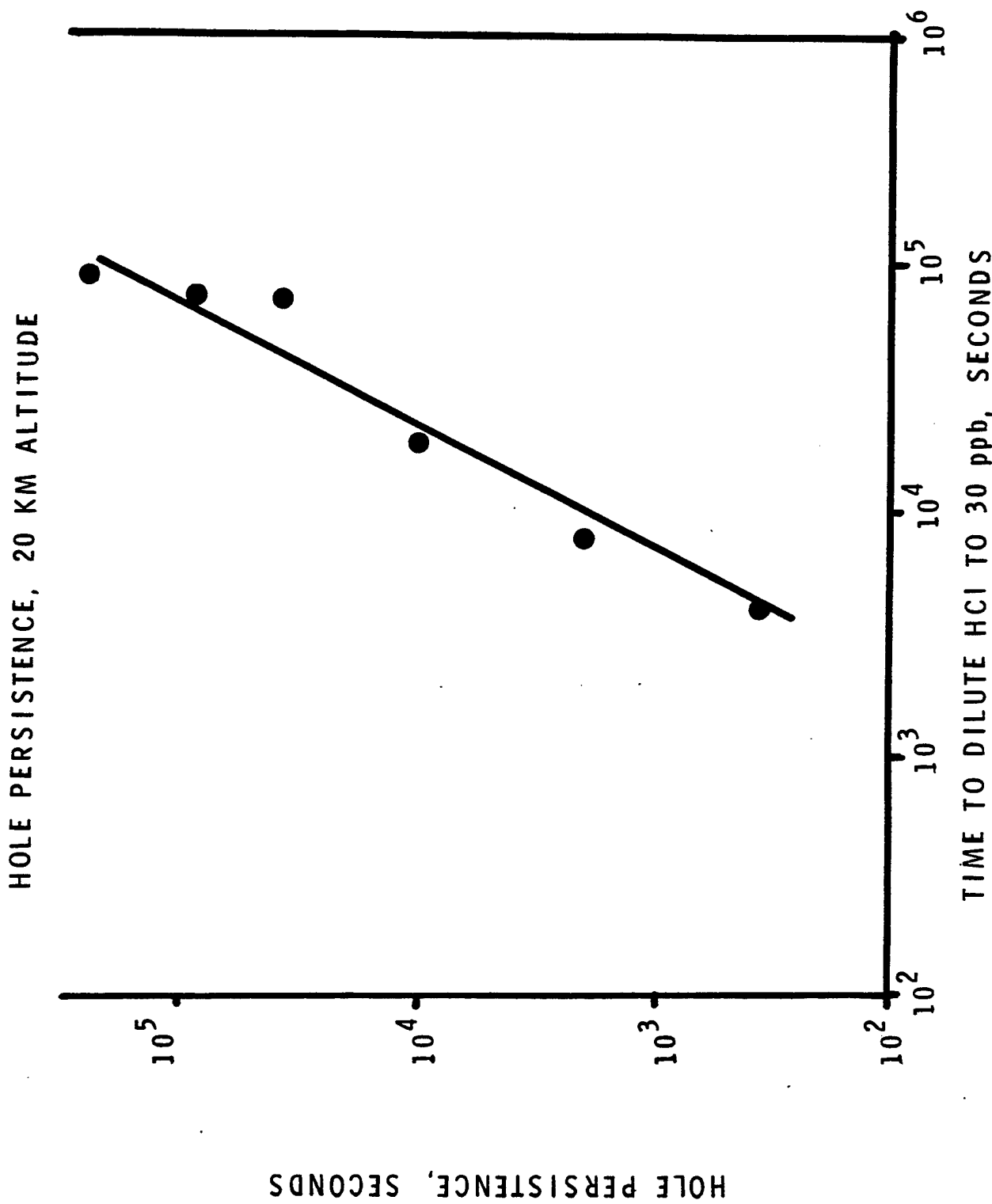


Figure 12. Ozone Hole Persistence as a Function of HCl Dissipation Time

APPROXIMATE HOLE SIZE, 20 KM ALTITUDE

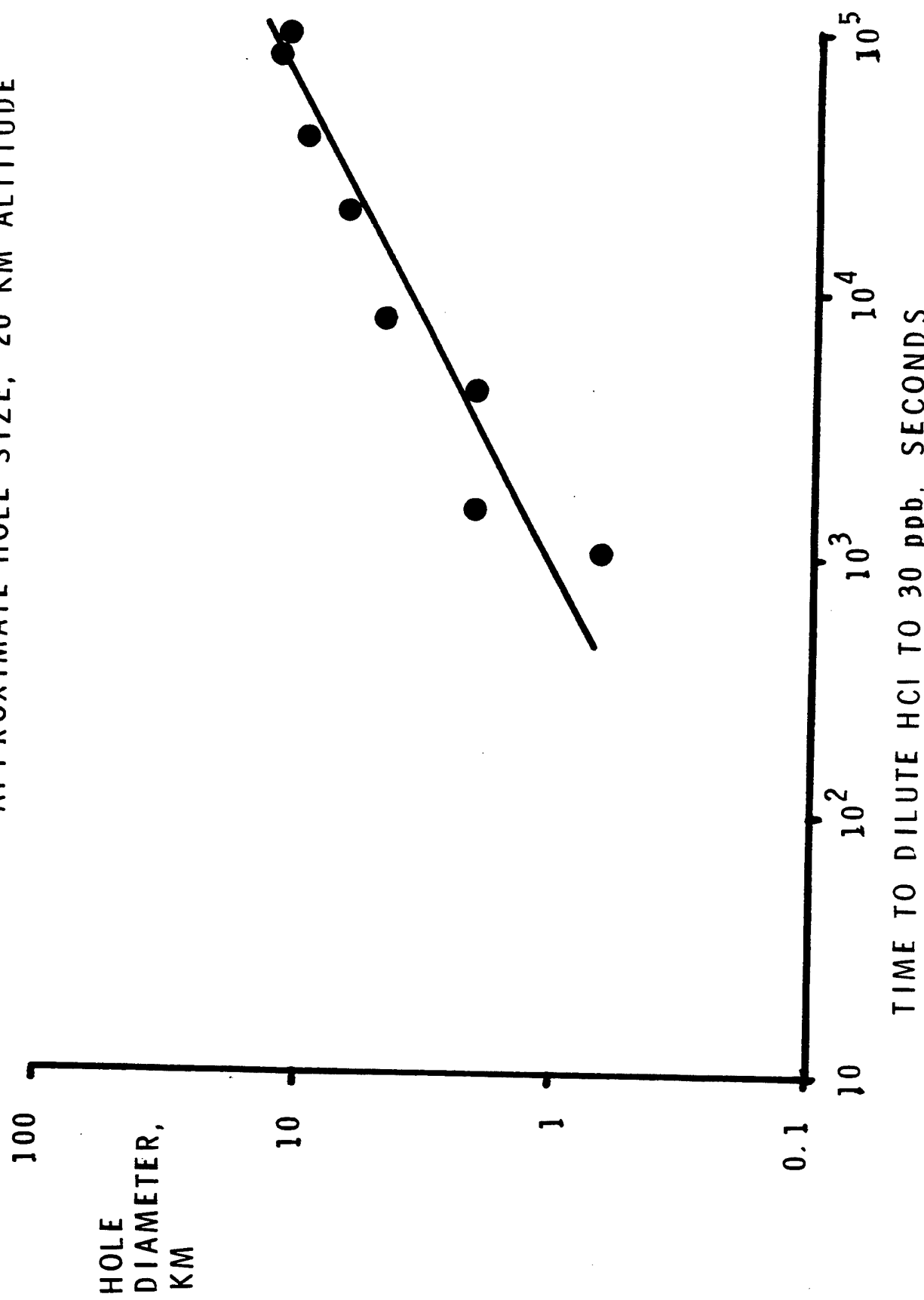


Figure 13. Ozone Hole Diameter as a Function of HCl Dissipation Time

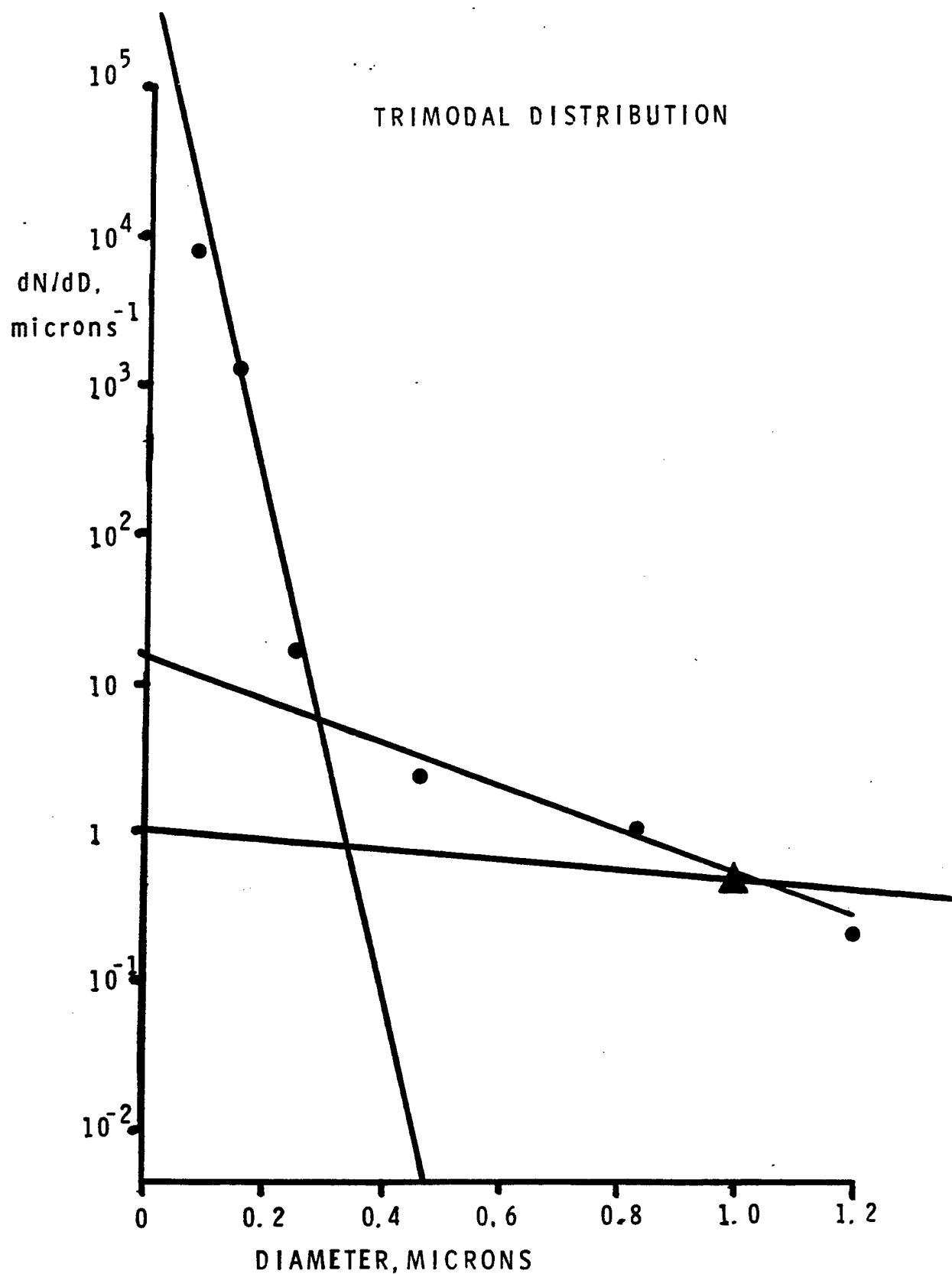


Figure 14. Trimodal Size Distribution of Alumina Particles

References

1. M. R. Denison, J. J. Lamb, W. D. BJORNDAL, E. Y. Wong, and P. D. Lohn, "Solid Rocket Exhaust in the Stratosphere: Plume Diffusion and Chemical Reactions," *J. Spacecraft and Rockets* **31**, 435–442 (1994).
2. I. L. Karol, Y. E. Ozolin, and E. V. Rozanov, "Effect of Space Rocket Launches on Ozone," *Ann. Geophysicae* **10**, 810–814 (1992).
3. B. C. Kruger, M. M. Hirschberg, and P. Fabian, "Effects of Solid-Fueled Rocket Exhausts on the Stratospheric Ozone Layer," *Ber. Bunsenges. Phys. Chem.* **96**, 268–272 (1992).
4. M. Yu. Danilin, "Local Stratospheric Effects of Solid-Fueled Rocket Emissions," *Ann. Geophysicae* **11**, 828–836 (1993).
5. P. F. Zittel, "Computer Model Predictions of the Local Effects of Large, Solid-Fuel Rocket Motors on Stratospheric Ozone," Aerospace Report No. TR-94(4231)-9, 10 September 1994.
6. L. R. Martin, "Possible Effect of the Chlorine Oxide Dimer on Transient Ozone Loss in Rocket Plumes," Aerospace Report No. TR-94(4231)-1, 15 March 1994.
7. H. S. Pergament, R. I. Gomberg, and I. G. Poppoff, "NO_x Deposition in the Stratosphere from the Space Shuttle Rocket Motors," pp. G-1 through G-5, Proceedings of the Space Shuttle Environmental Assessment Workshop on Stratospheric Effects, JSC-11633, NASA TM X-58198, January 1977.
8. M. E. Coltrin, R. J. Kee, and F. M. Rupley, (1991) SURFACE CHEMKIN (Version 4.0): A Fortran Package for Analyzing Heterogeneous Chemical Kinetics at a Solid-Surface—Gas-Phase Interface, *Sandia Report* SAND90-8003B. UC-401, 91pp.
9. R. J. Kee, F. M. Rupley, and J. A. Miller, (1991a) The Chemkin Thermodynamic Data Base, *Sandia Report* SAND87-8215B. UC-4, 155 pp.
10. R. J. Kee, F. M. Rupley, and J. A. Miller, (1991b) Chemkin-II: A Fortran Chemical Kinetics Package for the Analysis of Gas-Phase Chemical Kinetics, *Sandia Report* SAND89-8009. UC-401, 127 pp.
11. R. T. Watson, P. E. Smokler, and W. B. DeMore, "An Assessment of an F₂ or N₂O₄ Atmospheric Injection From an Aborted Space Shuttle Mission," JPL Publication 77-81, 41 pp. (1977).
12. B. B. Brady, E. W. Fournier, L. R. Martin, and R. B. Cohen, "Stratospheric Ozone Reactive Chemicals Generated by Space Launches Worldwide," Aerospace Report No. TR-94(4231)-6, June 1994, 23 pp.

14. W. R. Cofer, G. G. Lala, and J. P. Wightman, "Analysis of Mid-Tropospheric Space Shuttle Exhausted Aluminum Oxide Particles," *Atmospheric Environment* **21**, 1187–1196 (1987).
15. W. R. Cofer, G. C. Purgold, E. L. Winstead, and R. A. Edahl, "Space Shuttle Exhausted Aluminum Oxide: A Measured Particle Size Distribution," *J. Geophys. Res.* **96**, 17,371–17,376 (1991).
16. H. O. Kim, D. Laredo, and D. W. Netzer, "Measurement of Submicrometer Al_2O_3 Particles in Plumes," *Applied Optics* **32** 6834–6840 (1993).
17. E. J. Beiting, "Characteristics of Alumina Particles from Solid Rocket Motor Exhaust in the Stratosphere," Aerospace Report No. TR-95(5231)-8, 15 September 1995, 40 pp.
18. E. J. Beiting, "In-Situ Stratospheric Ultraviolet Absorption and Extinction Measurements in a Titan IV Plume," Aerospace Report No. ATM 94(4448)-7, June 1994, 30 pp.
19. M. K. W. Ko, N-D Sze, and M. J. Prather, "Better Protection of the Ozone Layer," *Nature* **367**, 505–508 (1994).
20. M. J. Molina, et. al., "Quantum Yield of Chlorine-Atom Formation in the Photodissociation of Chlorine Peroxide (ClOOCCl) at 308 nm," *Chemical Physics Letters* **173**, 310–315 (1990).
21. R. A. Cox and G. D. Hayman, "The Stability and Photochemistry of Dimers of the ClO Radical and Implications for Antarctic Ozone Depletion," *Nature* **332**, 796–800 (1988).
22. I. J. Eberstein, "Photodissociation of Cl_2O_2 in the Spring Antarctic Lower Stratosphere," *Geophys. Res. Letters* **17**, 721–724 (1990).
23. T. K. Minton, C. M. Nelson, T. A. Moore, M. Okumura, "Direct Observation of ClO from Chlorine Nitrate Photolysis," *Science* **258**, 1342–1345 (1992).
24. J. M. Rodriguez, "Probing Stratospheric Ozone," *Science* **261**, 1128–1129 (1993).

Appendix A

Estimate of the Surface Area of the Particles

The heterogeneous reactivity of the alumina particles will be proportional to the surface area available per unit volume of air and the sticking coefficient for the reaction in question, according to the standard kinetic theory result:

$$\frac{dn}{dt} = n \bar{v} \gamma A / 4$$

where n is the concentration of the reacting species in molecules/cm³, \bar{v} is the molecular velocity, γ is the sticking coefficient, and A is the available surface area per unit volume in cm²/cm³. The area, in turn, will be determined by the size distribution of the alumina particles and their shape. For our purposes, these properties may be summarized as an available surface area per gram of the alumina, which can then be put into our model. We know the mass of alumina released per unit altitude for the various launch systems (Ref. 12), and this can be combined with a dispersion model to give an absolute value for the surface area per unit volume of the atmosphere in the plume.

Atmospheric measurements of the alumina particles have been done by Strand, et. al. (Ref. 13), and by Cofer, et. al., (Refs. 14, 15), with some recent laboratory studies by Kim, et. al. (Ref. 16). A detailed discussion of the particle size distributions has been recently given by Beiting (Ref. 17). The work by Beiting includes the possibility of a variation of the size distribution with position in the plume. In our calculations, we are not including this effect.

The measurements by Strand, et. al., were done at 20 km altitude, and the measurements by Cofer, et. al., at altitudes up to 7 km. Cofer's work clearly shows that the particles are spherical, so the surface area of each particle is simply:

$$a = \pi D^2$$

where D is the diameter of the particle. For a given size distribution dN/dD , the total number, N , the total area, A , and the total volume, V , will be given respectively by:

$$N = \int (dN/dD) dD$$

$$A = \int \pi D^2 (dN/dD) dD$$

$$V = \int (\pi/6) D^3 (dN/dD) dD$$

where the integrals are over the size limits of the distribution function. Examination of the literature data on the size distribution shows that a single function for dN/dD is not adequate to represent the data. Instead we will use three distributions for three different size ranges covered by the data. The

work by Strand, et. al., covers sizes from 0.02 to 3 microns, and requires two distribution functions. The work by Cofer, et. al., covers roughly 1 to 10 microns, and requires a third function. We will arbitrarily match the Cofer and Strand distributions at 1.0 micron. The discussion by Beiting (Ref. 17) gives arguments justifying a match of the two papers at this point. For convenience, we will put everything in terms of simple exponential distributions. To do this required re-plotting and fitting the raw data of Strand, et. al., and this is shown in Figure 14. The distribution of Cofer, et. al., is used as quoted in the paper (noting a typographical error in the paper.) The composite fit to the data is as follows:

0.02 to 0.30 microns diameter:

$$dN/dD = 4.1 \times 10^5 e^{-40D}$$

0.30 to 1.0 microns diameter:

$$dN/dD = 18.4 e^{-3.5D}$$

1.0 to 10 microns diameter:

$$dN/dD = 1 e^{-0.89D}$$

The composite distribution has the following properties when integrated over the respective size intervals (normalized to one large particle):

Small mode: $N_1 = 2.21 \times 10^4$, $D_1 = 0.025$ microns (80% of surface area)

Medium mode: $N_2 = 3.64$, $D_2 = 0.552$ microns (3% of surface area)

Large mode: $N_3 = 1$, $D_3 = 2.39$ microns (17% of surface area)

The literature suggests a value for the density of the particles of 2.0 gm/cm^3 (instead of 4.0 for pure alumina). This gives for a final value of area-to-mass ratio:

$$A/M = 4.4 \times 10^4 \text{ cm}^2/\text{gm, or } 4.4 \text{ meters}^2/\text{gm}$$

One final step is necessary. SURFACE CHEMKIN is set up to work with a monodisperse aerosol, so we replaced the above distribution with a monodisperse distribution of pure alumina ($\rho = 4.0$) with an equivalent surface/mass ratio. This aerosol has a uniform diameter of:

$$D = 0.34 \text{ microns.}$$